

Dominant two-center electron-electron interactions in collisions of 120-MeV Ne^{6+} ions with gas targets

B. Sulik, S. Ricz, and I. Kádár

Institute of Nuclear Research of the Hungarian Academy of Sciences, P.O. Box 51, H-4001 Debrecen, Hungary

G. Xiao, G. Schiwietz, K. Sommer, P. Grande, R. Köhrbrück, M. Grether, and N. Stolterfoht
Hahn-Meitner-Institute, Glienicke Strasse 100, D-14109 Berlin, Germany

(Received 8 August 1994; revised manuscript received 8 March 1995)

The target gases H_2 , He, CH_4 , N_2 , Ne, and Ar were bombarded by 120-MeV Ne^{6+} ions to study the $2s$ - nl excitation from the metastable state $1s^2 2s 2p^3 P_0$ of the Ne^{6+} projectile. The Coster-Kronig electrons from the transition $1s^2 2pnl$ ($n \geq 7$) $- 1s^2 2s + e^-$ were measured using the method of zero-degree electron spectroscopy. It was found that the production cross section for the Coster-Kronig electrons is roughly proportional to the target atomic number. The experimental data are in agreement with impact-parameter calculations, which take into account the quenching of the 3P_0 metastable state of the projectile, by exciting or ionizing its $2p$ electron. This agreement supports the conclusion that the dielectronic two-center process is dominant in the production of Coster-Kronig electrons following the $2s$ - nl excitation of the projectile by H_2 and He targets ($> 56\%$), and remains significant for the other investigated targets ($> 22\%$).

PACS number(s): 34.50.Fa

INTRODUCTION

When both partners carry electrons into an atomic collision, the Coulomb field of the nuclei may strongly be screened provided the electrons remain in their ground state during the collision. Screening effects can significantly reduce the cross section of inelastic processes. However, inelastic processes may be enhanced by the mutual collision of projectile and target electrons, when the repulsion between the electrons changes their states during the collision. This latter process is referred to as the dielectronic two-center process [1]. It has often been denoted as antiscreening in the literature [2]. Both collisional screening effects and dielectronic two-center processes are manifestations of the interactions between projectile and target electrons [3]. They are treated first by Bates and Griffing [4] for $\text{H}+\text{H}$ collisions within the framework of the plane-wave Born approximation (PWBA). Similar studies have been performed by several authors (e.g., [2,5–9]). Two-center electron-electron interactions are particularly important in projectile spectroscopy, where the projectile ion is excited or ionized by a neutral target atom.

Contrary to the early theoretical studies [4], the detailed experimental investigations of dielectronic two-center processes have been performed only recently. In high-energy atomic collisions, evidence for dielectronic two-center processes has been provided by Zouros, Lee, and Richard [10] and Hülskötter *et al.* [11]. Recently, in accordance with theory, it has been demonstrated in many collision systems that dielectronic processes yield a large contribution to electron loss [12–14] and excitation of the projectile [14]. DuBois and Manson [5] studied ionization of the target by neutral H and He projectiles. They have found that the production of low-energy elec-

trons emitted from the target outer shells is mainly due to dielectronic two-center processes.

In the present study, we investigate a collision process where the contribution of the dielectronic interaction is shown to be larger than that of the screened nuclear charge. According to the analysis given by Briggs and Taulbjerg within the PWBA framework [5], dielectronic two-center processes are expected to be dominant for excitations associated with small energy and momentum transfer, i.e., for distant and fast collisions. In distant collisions the nucleus of a neutral target atom can be almost completely screened and target electrons may enter as the most effective agents in exciting or ionizing the projectile.

For the electron-loss process of the projectile, the conditions of low-energy transfer are fulfilled when the ejected electrons are slow in the projectile frame of reference. Here, in principle, one may investigate the electron-loss peak around 0° . For the present study, we selected an excitation of the $2s$ electron in a Ne^{6+} projectile ion into a high-lying Rydberg state ($n \geq 7$). This type of transition better fulfills the condition of low-energy transfer. Moreover, the theoretical descriptions of the screening and dielectronic contributions can be handled more easily for bound than for continuum final states. In this work, we performed calculations in the first-order Born approximation and, to take into account higher-order processes, in the framework of the impact-parameter treatment.

In the present study, we measured the $2s$ - nl excitation cross sections primarily for hydrogen and helium targets. Our PWBA calculations predict a larger cross section for H_2 than for He. This is due to the fact that in the dielectronic process the two loosely bound electrons of the H_2 molecule are more effective exciting agents than the more tightly bound electrons of He. The main purpose of the

experimental work was to confirm that the measured cross section for H_2 was significantly larger than that for He. This would provide experimental evidence that dielectronic two-center processes are dominant for the investigated collision system. In order to explore the studied process in a wider range of collision parameters, the experiments were extended to heavier targets.

EXPERIMENTAL METHOD

The experimental study of the transition from an outer shell to a Rydberg state was performed by measuring the Coster-Kronig (CK) electrons

$$1s^2 2pnl (n \geq 7) \rightarrow 1s^2 2s + e^- (\text{CK}),$$

which were emitted following the $2s-nl$ excitation of Ne^{6+} projectiles in the metastable state $1s^2 2s 2p^3 P_0$,

$$1s^2 2s 2p^3 P_0 \rightarrow 1s^2 2pnl (n \geq 7).$$

In the experiments, different targets (H_2 , He, CH_4 , N_2 , Ne, and Ar) in a gas cell were bombarded by 120-MeV Ne^{6+} ions at a beam line of the Ionenstrahllabor (ISL) accelerator facility at Hahn-Meitner-Institute in Berlin. The ejected electron spectra were acquired by a tandem electron spectrometer at 0° relative to the beam direction. The experimental arrangement was the same as that given in Ref. [16], so that only a few details shall be given here. The metastable fraction of the beam was close to 50% [17]. It was estimated that the contribution to the same excited state by double excitation ($2s-2p$ and $2s-nl$) of incident ground-state ions is not significant. Our impact-parameter calculations (see below) yielded only a 2% effect for this process.

The absolute target pressure in the gas cell, i.e., the number density of the target atoms or molecules, was directly measured in the gas cell by means of a membrane-type Baratron pressure sensor. It was kept constant by a regulated valve. Therefore the relative cross sections for different targets could be determined. In order to check the single collision condition we performed the measurements with different target pressures from 5×10^{-3} to 9×10^{-2} mbar. No pressure dependence was found in the measured excitation cross sections.

Figure 1 displays the electron spectra obtained with H_2 and He targets. The Coster-Kronig peak groups are located on the two wings of the electron-loss peak. The intensity of a Coster-Kronig peak group for a given n at 0° is proportional to a linear combination of the $2s-nlm$ excitation cross sections [see Eq. (3) below]. It is clearly seen that for the H_2 target the spectrum is larger in intensity than that for the He target at the same target cell pressure, in agreement with the PWBA prediction. This is true not only for the Coster-Kronig peaks but also for the measured region of the electron-loss peak.

In the present work, our attention is focused on the relative cross sections for producing the $n=7$ final state (i.e., the two most intense line groups). Besides $n=7$, $n=8$ and 9 were also analyzed. For all three n values the relative yields were found to be equal, within the experimental uncertainties. Therefore, we performed a detailed

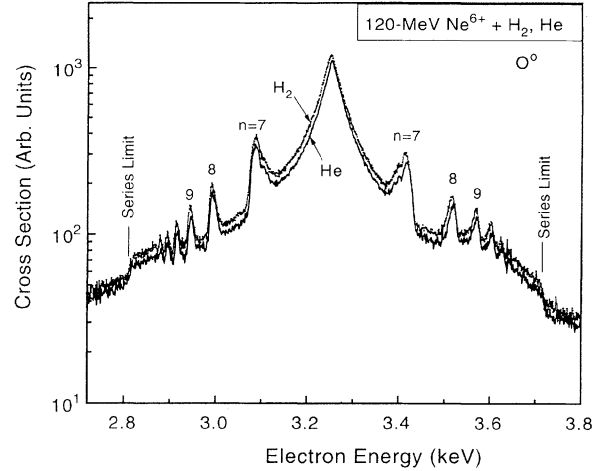


FIG. 1. Electron spectra measured at 0° in 120-MeV $Ne^{6+} + H_2$ and $Ne^{6+} + He$ collisions with the same target pressure (5.3×10^{-2} mbar) in the gas cell. The spectra show Coster-Kronig groups, due to the initial configuration $1s^2 2pnl$ where n is indicated.

analysis only for $n=7$. The line-group intensities have been evaluated after transforming the spectra into the projectile frame of reference and subtracting the background. This way, we obtained relative yields for electron emission in the projectile frame, proportional to the corresponding differential cross sections. These quantities were compared with the theory. The relative yields at 0° and 180° were found to be equal, within experimental uncertainties.

THEORETICAL METHODS

Within the framework of PWBA [2,5,9], the screening and dielectronic contributions to a projectile excitation $i \rightarrow f$ are expressed as follows. Hereafter, the target is considered to be a neutral atom. Throughout this paper, atomic units ($m_e = e = \hbar = 1$) are used

$$\sigma_{if}^{\text{scr}} = \frac{8\pi}{v^2} \int_{q_{\min}}^{\infty} \frac{dq}{q^3} |F_{if}^{(P)}|^2 [Z_T - F_{00}^{(T)}]^2, \quad (1)$$

$$\sigma_{if}^{\text{diel}} = \frac{8\pi}{v^2} \int_{q_{\text{eff}}}^{\infty} \frac{dq}{q^3} |F_{if}^{(P)}|^2 S_T. \quad (2)$$

Here v is the projectile velocity and Z_T is the target atomic number (which is equal to the number of electrons for neutral targets). The projectile and target form factors are denoted by $F^{(P)}$ and $F^{(T)}$, respectively. Within the framework of the independent-particle model, the elastic form factor of the target can be considered as a sum of one-electron elastic form factors [9]. The inelastic scattering function is an infinite sum of the squared absolute values of all the inelastic target form factors. It is usually estimated with the help of the closure approximation [2,5,9]. For the screening contribution, $q_{\min} = (E_f - E_i)/v$. For the dielectronic contribution, q_{eff} is calculated by means of the Bethe sum-rule method in

Ref. [9].

The total cross section for the $2s-nlm$ transition σ_{2s-nlm} was calculated as the sum of the screening and dielectronic contributions. For a given n , the total cross section σ_{2s-n} was obtained by summing over all the possible l and m quantum numbers.

When applying the LS coupling scheme, only the final states with $M=0$ will contribute to the Coster-Kronig

electron emission at 0° . The $2p$ electron has an angular momentum of $l'=1$. As the metastable fraction of the beam is nonpolarized, the occupation probabilities of the magnetic quantum numbers $m'=-1, 0, \text{ or } 1$ of the $2p$ electron are equal ($p=\frac{1}{3}$). Since $m+m'=M=0$, the single differential cross section for electron emission at 0° (i.e., the quantity that is comparable to the experimental yield) was calculated as follows:

$$\frac{d\sigma_{2s-n}}{d\Omega}(0^\circ) = \frac{1}{3} \frac{1}{4\pi} \sum_{l=0}^{n-1} \sum_{m=-1}^1 \sigma_{2s-nlm} \sum_{L=|l-1|}^{l+1} (2L+1) |\langle 1, -m; l, m | L, 0 \rangle|^2. \quad (3)$$

In the PWBA calculation is, Hartree-Fock wave functions were determined by means of the Froese Fischer code [18,19] to provide the projectile form factors and the energies of the ionic states E_i and E_f . The Hartree-Fock elastic form factors for the target atoms were taken from the table of Hubbell *et al.* [20]. For calculating the dielectronic part, we utilized the inelastic scattering function S_T , also tabulated by Hubbell *et al.* [20], which contains the correction terms belonging to the forbidden transitions for many-electron atoms.

Since the table in Ref. [20] contains the data for both atomic and molecular hydrogen, as well as hydrogen atoms in C—H bonded situations, we performed calculations for an individual H atom, for a H atom in a H_2 molecule, and for a H atom in a C—H bond. It was found that the difference between H atoms bonded in the H_2 and CH_4 molecule is negligible for the present collision system. However, the cross section for an individual H atom was found to be 10% larger than that for the H atom bonded in the H_2 molecule. This result is similar to the experimental finding of Pedersen and Larsen [21] for the ionization of He by H and H_2 at large impact velocities.

In the following, we consider the above PWBA cross sections as theoretical first-order results for the corresponding Coster-Kronig emission cross sections. The PWBA cross section for a H atom bond in the H_2 molecule is considered as the calculated hydrogen result.

To analyze the collision system in more detail, i.e., to take into account multiple processes at heavier targets, we performed calculations using an impact-parameter treatment [22]. Within the impact-parameter calculations the target was modeled in an approximate manner, i.e., all the target electrons were characterized by a single hydrogenic $1s$ -type wave function with a common effective atomic parameter a [22]. In order to provide equivalent PWBA and impact-parameter treatments, we performed a corresponding set of PWBA calculations by means of the above simplified model for the target. The atomic parameters were chosen to reproduce the accurate PWBA screening cross sections for every target species. This way, we set the proper effective $1s$ atomic parameter values for the impact-parameter calculations (see below).

It was found that the accurate dielectronic PWBA con-

tributions were also quite well reproduced (within 2%) by the above simplified calculations for the target atoms H and He. For heavier targets the simplified calculations provided a larger dielectronic contribution than the accurate PWBA. The difference amounts to 20% for the Ar target. In the following, we use the simplified PWBA calculations as a reference for comparison with the impact-parameter results. Hereafter, the set of the simplified PWBA calculations will be referred to as SPWBA.

Within the framework of the impact-parameter treatment, the cross section of a transition reads

$$\sigma_{if} = 2\pi \int_0^\infty db b p_{if}(b). \quad (4)$$

In a test-set of the impact-parameter calculations, we calculated the probabilities

$$p_{2s-nlm} = P_{2s-nlm}^{\text{scr}} + p_{2s-nlm}^{\text{diel}}$$

within the framework of the first-order semiclassical approximation. The screening term was evaluated by the method in Refs. [22,23] using Hartree-Fock projectile wave functions and a common hydrogenic $1s$ -type atomic parameter for all the target electrons [22]. As noted before, the atomic parameters belonging to the different targets were determined by the SPWBA set of calculations. The dielectronic probability term was evaluated by a method that is equivalent to that of Ref. [24]. The cross sections were found to be in accurate agreement with those calculated in the SPWBA set. This way, we verified the equivalence of the PWBA and impact-parameter calculations.

In the second set of impact-parameter calculations we evaluated the Coster-Kronig emission probabilities and cross sections by taking into account the quenching of the metastable state of the projectile. In the applied simple model, the excitation or ejection of the $2p$ electron, simultaneously with the $2s-nlm$ excitation, was considered as the most important quenching process. Thus, the impact-parameter-dependent probability of a particular $2s-nlm$ excitation, which can be followed by a Coster-Kronig transition, is obtained as

$$p_{2s-nlm}^{2p-2p} = p_{2s-nlm} (1 - p_{2p-\Sigma}), \quad (5)$$

where $p_{2p-\Sigma}$ is the total probability of removing the $2p$

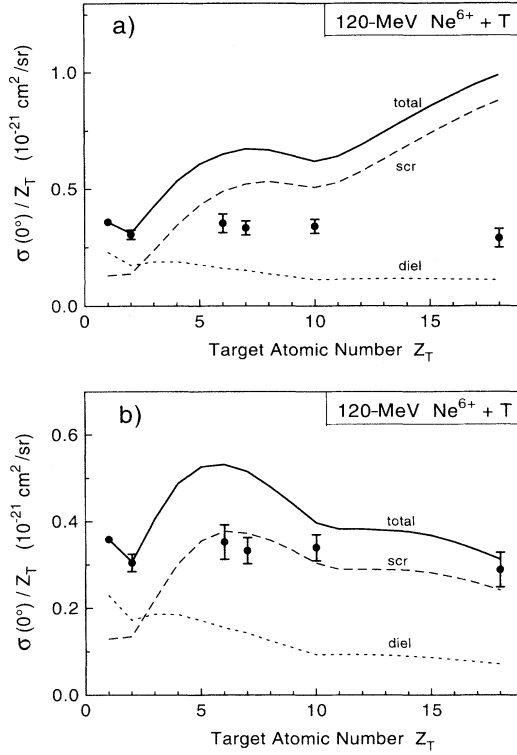


FIG. 2. Single differential Coster-Kronig emission cross sections for $n=7$ divided by the target atomic number Z_T . In (a) and (b), theoretical data are given without and with taking into account the quenching of the 2P_0 metastable state, respectively. Experiment: symbols with error bars. Theory: dashed line, screening contribution; dotted line, dielectronic contribution; full line, the sum of the two contributions. Experiment is normalized to theory at hydrogen ($\frac{1}{2}\text{H}_2$, see text).

electron from its initial state. During the calculations, $p_{2p-\Sigma}$ was approximated by its screening component. We had learned from the test-set of the impact-parameter calculations (see above) that the dielectronic probability term is much smaller than the screening term for the heavier ($Z \geq 6$) targets. The probability $p_{2p-\Sigma}^{\text{scr}}$ was determined by the same method that had been used in the

test-set of the impact-parameter calculations, but including 300 final states, and applying a first-Magnus correction [22]. We also calculated $p_{2s-\Sigma}^{\text{scr}}$ in the same way, in order to apply the first-Magnus correction for p_{2s-nlm} , too. The cross sections of this second set were calculated by means of Eqs. (3)–(5). For the dielectronic contribution, the ratios of the two sets of the impact-parameter results were used to correct the corresponding PWBA cross sections.

In Table I and Fig. 2, the PWBA results are displayed as theoretical Coster-Kronig emission cross sections without quenching correction, and the results, calculated by means of Eqs. (3)–(5), are displayed as those with quenching correction. The calculations have been performed not only for the measured systems, but for all the target atoms from $Z=1$ to 18. Finally, it should be noted that the results were found to be insensitive to the choice of coupling scheme, since the angular distribution of the Coster-Kronig emission, calculated within the framework of the LS coupling scheme [Eq. (3)], is not far from isotropy.

RESULTS AND DISCUSSION

In order to compare experiment and theory, the molecular targets were treated as a group of independent neutral atoms (except H_2). Hence, we reduced the measured data to cross sections per target atom; e.g., for N atoms, we divided the measured molecular cross sections by 2. For carbon, we subtracted the measured H_2 cross section twice from the CH_4 cross section. In contrast to hydrogen, there are no tabulated elastic form factor and inelastic-scattering-function values for the CH_4 and N_2 molecules.

The calculated and measured single differential cross sections for Coster-Kronig electron emission at 0° are presented in Fig. 2 and Table I. We normalized experiment to theory for hydrogen, i.e., for a H atom bond in the H_2 molecule. The quoted uncertainties contain the statistical error of the data and the measured (reproducibility) error of the target pressure in the gas cell. For graphical reasons, in Fig. 2, the cross sections are divided by the target atomic number.

TABLE I. Calculated and measured single differential Coster-Kronig emission cross sections at 0° in $10^{-21} \text{ cm}^2/\text{sr}$ units ($n=7$ group), with and without taking into account the quenching of the 3P_0 metastable state. The measured cross sections are normalized to the theory at the hydrogen target (H corresponds to $\frac{1}{2}\text{H}_2$; see text). Screening (scr) and dielectronic (diel) contributions to the total cross section (scr + diel) are also presented separately.

Target	Theory without quenching			Theory with quenching			Measured
	Scr	diel	scr + diel	scr	diel	scr + diel	
H	0.130	0.229	0.359	0.129	0.229	0.358	0.358 ^{a,b}
He	0.274	0.346	0.620	0.269	0.345	0.613	0.61 (4)
C	2.935	0.960	3.895	2.262	0.927	3.198	2.11 (23) ^a
N	3.640	1.064	4.704	2.604	0.997	3.601	2.33 (18) ^a
Ne	5.063	1.120	6.183	3.063	0.929	3.965	3.40 (27)
Ar	15.81	1.980	17.79	4.338	1.275	5.613	5.19 (68)

^aReduced values from the measured molecular data. See text.

^bNormalized to theory at this point.

The theoretical cross sections calculated without taking into account the quenching of the 3P_0 metastable state are compared with experiment in Fig. 2(a). There is an excellent agreement between experiment and the PWBA theory (solid curve, labeled "total") when going from hydrogen to helium. As noted above, the experimental results support the theoretical prediction that the dielectronic contribution (dotted line, labeled "diel") dominates the screening contribution (dashed line, labeled scr) for H_2 and He. For heavier targets, the agreement breaks down. Contrary to the experimental results, PWBA predicts a more steeply increasing cross section with the target atomic number.

When taking into account the quenching of the 3P_0 metastable state, one finds a significant change in the theoretical data. Figure 2(b) shows that there is a general agreement between experiment and theory for the molecular hydrogen and the investigated inert gas targets. For C and N, the reason for the remaining disagreement may be due to the open-shell structure and/or the bonding of the target atoms. For the hydrogen and helium targets, quenching of the metastable states has been found to be negligible. According to the calculations, the quenching effect is significantly smaller for the dielectronic contribution as it is more delocalized in space. Therefore, the dielectronic contribution to the Coster-Kronig emission is either dominant (> 50%) or significant (> 20%) for all the investigated targets. The agreement between experiment and theory supports the conclusion that the most important features are properly accounted for by the present model.

An interesting finding is that the measured single differential cross sections are nearly proportional to the target atomic number. It is clearly seen in Fig. 2, where the experimental data form an almost horizontal line. This can be considered as an accidental result from the competition between the excitation mechanisms involving the $2s$ and $2p$ subshells of the projectile.

It is concluded that the measured cross sections for H_2 and He provide evidence for an inelastic atomic collision process that is dominated by dielectronic two-center processes. The electrons of a light target screen the field of the target nucleus strongly and take the role of the active agents. For heavier targets, the measured Coster-Kronig emission cross section was found to be nearly proportional to the target atomic number. The present model, which takes into account the quenching of the 3P_0 metastable state of the projectile by exciting or ionizing its $2p$ electron, provides general agreement between experiment and theory also for the heavier targets. The agreement supports that the dielectronic contribution to the Coster-Kronig electron emission remains significant for all the investigated targets.

ACKNOWLEDGMENTS

This work was supported by the German-Hungarian Collaboration in Science and Technology (Project No. 75), by the Hungarian Academic Research Fund (AKA, Contract No. 1-300-2-91-0-790), and by the Hungarian National Science Fund (Contract Nos. OTKA-3011 and OTKA-T-014-323).

- [1] N. Stolterfoht, Nucl. Instrum. Methods B **53**, 477 (1991).
- [2] J. H. McGuire, N. Stolterfoht, and P. R. Simony, Phys. Rev. A **24**, 97 (1981).
- [3] N. Stolterfoht, in *Spectroscopy and Collisions of Few Electron Ions*, edited by M. Ivascu, V. Florescu, and V. Zoran (World Scientific, Singapore, 1989), p. 342.
- [4] D. R. Bates and G. Griffing, Proc. Phys. Soc. London Sec. A **66**, 961 (1953); **67**, 663 (1954).
- [5] J. S. Briggs and K. Taubjerg, in *Structure and Collisions of Ions and Atoms*, edited by I. A. Sellin (Springer-Verlag, Berlin, 1978), p. 105.
- [6] K. L. Bell, V. Dose, and A. E. Kingston, J. Phys. B **2**, 831 (1969); K. L. Bell and A. E. Kingston, *ibid.* **4**, 162 (1971).
- [7] S. T. Manson and L. H. Toburen, Phys. Rev. Lett. **46**, 529 (1981).
- [8] R. Anholt, Phys. Lett. **114A**, 126 (1986).
- [9] E. C. Montenegro and W. E. Meyerhof, Phys. Rev. A **43**, 2289 (1991).
- [10] T. J. M. Zouros, D. H. Lee, and P. Richard, Phys. Rev. Lett. **62**, 2261 (1989).
- [11] H. P. Hülskötter, W. E. Meyerhof, E. D. Dillard, and S. T. Guardola, Phys. Rev. Lett. **63**, 1938 (1989).
- [12] H.-P. Hülskötter, B. Feinberg, W. E. Meyerhof, A. Belkacem, J. R. Alonso, L. Blumenfeld, E. A. Dillard, H. Gould, N. Guardala, G. F. Krebs, M. A. McMahan, M. E. Rhoades-Brown, B. S. Rudde, J. Schweppe, D. W. Spooner, K. Street, P. Thieberger, and H. E. Wegner, Phys. Rev. A **44**, 1712 (1991).
- [13] D. H. Lee, T. J. M. Zouros, J. M. Sanders, P. Richard, J. M. Anthony, Y. D. Wang, and J. H. McGuire, Phys. Rev. A **46**, 1374 (1992).
- [14] T. J. M. Zouros, D. H. Lee, J. M. Sanders, and P. Richard, Nucl. Instrum. Methods B **79**, 166 (1993).
- [15] R. D. DuBois and Steven T. Manson, Nucl. Instrum. Methods B **86**, 161 (1994).
- [16] A. Itoh, D. Schneider, T. Schneider, T. J. M. Zouros, G. Nolte, G. Schiwietz, W. Zeitz, and N. Stolterfoht, Phys. Rev. A **31**, 684 (1985).
- [17] N. Stolterfoht, Phys. Rep. **146**, 401 (1987).
- [18] Charlotte Froese Fisher, *The Hartree-Fock Method for Atoms* (Wiley, New York, 1977).
- [19] Charlotte Froese Fisher, U. S. Department of Energy, Report No. ER/10618-11, 1983 (unpublished).
- [20] J. H. Hubbell, Wm. J. Veigele, E. A. Briggs, R. T. Brown, D. T. Cromer, and R. J. Howerton, J. Phys. Chem. Ref. Data **4**, 471 (1975).
- [21] E. Horsdal Pedersen and Lea Larsen, J. Phys. B **12**, 4099 (1979).
- [22] G. Schiwietz and P. L. Grande, Radiat. Eff. Solids **130-131**, 137 (1994).
- [23] S. Ricz, B. Sulik, N. Stolterfoht, and I. Kádár, Phys. Rev. A **47**, 1930 (1993).
- [24] E. C. Montenegro and W. E. Meyerhof, Phys. Rev. A **46**, 5506 (1992).